Hierarchical Forecasting for the Management of Distribution Grids

Simon Camal, Dennis van Der Meer, Fabrizio Sossan, Georges Kariniotakis

HIERARCHICAL FORECASTING FOR THE MANAGEMENT OF DISTRIBUTION GRIDS

Simon CAMAL
Mines PARIS – PSL University
Centre PERSEE, Sophia Antipolis, France
simon.camal@minesparis.psl.eu

Dennis VAN DER MEER
Mines PARIS – PSL University
Centre PERSEE, Sophia Antipolis, France
dennis.van_der_meer@minesparis.psl.eu

Fabrizio SOSSAN
HES-SO Valais Wallis
Institut de Recherche Energie et Environnement
fabrizio.sossan@hevs.ch

George KARINIOTAKIS
Mines PARIS – PSL University
Centre PERSEE, Sophia Antipolis, France
georges.kariniotakis@minesparis.psl.eu

ABSTRACT

The various voltage levels of power systems form a hierarchical structure. In radial distribution grids, the individual production or consumption of Distributed Energy Resources (DER) operating at the low voltage or medium voltage flow through the grid, experiencing losses and constraints, before summing up at the substation transformer which constitutes the TSO/DSO interface. Considering that most of these resources are operated by different stakeholders issuing independent energy forecasts, this work proposes a reconciliation approach to predict Photovoltaics (PV) production in distribution grids. The impact of reconciliation is analysed in terms of prediction error at the PV site, but also in terms of estimation of the aggregated flow at the TSO/DSO interface and the associated flexibility map in active/reactive power of DER operating in a selected Medium Voltage (MV) grid.

INTRODUCTION

Hierarchical forecasting (HF) is an appealing technique to generate forecasts of load or RES at multiple voltage levels. HF derives forecasts that are coherent throughout the hierarchy: for deterministic forecasts, this means that the sum of forecasts obtained at the bottom nodes of the hierarchy equals the forecast of the total load or RES production at the top of the hierarchy. HF provides information about the marginal contribution of each bottom node to the aggregated power estimate, without the inconsistency that is commonly observed when separate models are built for the various nodes of the hierarchy. Another advantage of HF lies in its capacity to reduce forecasting errors, including at the top node of the hierarchy.

Applications of hierarchical forecasting have been proposed in the context of wind generation to forecast the aggregated power output of wind farms [1] and for power demand in distribution grids [2]. This work presents the solutions developed in the frame of the H2020-RIA project Smart4RES [3] to produce a hierarchical forecast of distributed energy resources (DER) operating in distribution grids. The considered use case applies HF on PV sites that operate in different LV grids under the same MV network (cf. Figure 1). HF is derived through forecast reconciliation, which corresponds to a realistic case where independent forecasts are issued at the different LV nodes. This may originate from the fact that forecasts are obtained by a model which is not taking into account spatial dependencies, or that PV sites are operated by different owners who prefer to run their own forecasting models.

In the context of predictive management of distribution grids, forecasts are needed to estimate the flexibility that integrated DER can provide within a given grid [4]. In order to accurately quantify the flexibility potential of a MV grid, the adequate number of DER scenarios required by a robust optimization is discussed in [5]. However, the existing literature is scarce on the potential benefit of deploying specific forecasting solutions for the quantification of flexibility.

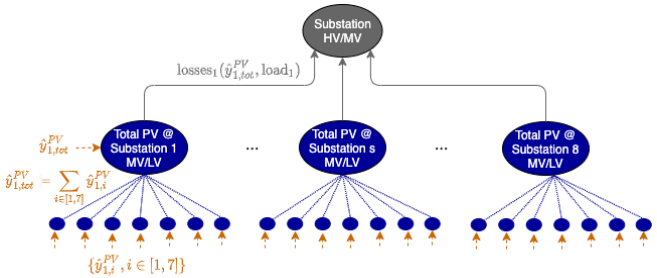

Figure 1: Use Case for hierarchical forecasting: reconciliation of PV forecasts is applied to each hierarchy formed by the PV sites operating under a given MV/LV substation. The MV grid contains 8 LV grids with identical topology, each of which with 7 PV plants. The total PV production predicted at each MV/LV substation is fed into a power flow simulation of the MV grid

METHODOLOGY

Overview

The proposed approach is composed of a sequence of four methodological steps (cf. Figure 2). The first two consist

in the derivation of independent forecasts at each node of the LV grids (called hereafter 'base' i.e. unreconciled), then these forecasts are reconciled. In the following steps, the predicted forecasts (base and reconciled) are fed into a power flow to quantify flows within the MV network, including the different LV grids. Finally, the influence of the PV forecast on the net-load estimation at the MV/HV connection is analyzed, and the extension to an estimate of the flexibility potential via Optimal Power Flow is discussed.

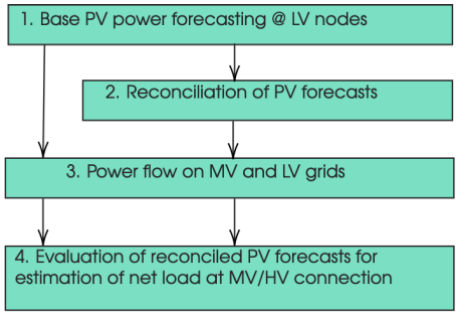

Figure 2: Methodological workflow

Reconciliation of hierarchical forecasts

First, base hierarchical forecasts are derived by regression models fitted on each PV site and on the total PV production of each LV grid. Two alternative regression models are tested, namely Lasso and Random Forest (RF), corresponding to the state-of-the-art in PV forecasting [6]. Models are built for each horizon between 15 minutes and 6 h ahead (24 horizons of 15 minutes). This horizon range is deemed representative of horizons chosen by Distribution System Operators (DSO) to manage local flexibilities after energy offers have been fixed on the day-ahead market. At these horizons, the most explanatory variables are recent past levels of PV production that are heavily influenced by the deterministic trend linked to the clear-sky (CS) irradiance potential. In what follows, a normalization of PV power using the CS method of [7] is applied to all models.

Then, five different reconciliation methods are applied to obtain coherent forecasts at each horizon h, i.e. that the sum of individual PV forecasts equal the forecast of the total PV production. The general approach is to derive a reconciliation matrix β_h that derives in (1) the reconciled prediction vector $\tilde{y}_h := (\tilde{y}_{tot}, \tilde{y}_1, \dots, \tilde{y}_P)$ from a projection of the base prediction vector $\hat{y}_h := (\hat{y}_{tot}, \hat{y}_1, \dots, \hat{y}_P)$, where P is the number of PV sites, y_{tot} is the total PV production and S the summation matrix. Please refer to [1]-[2] for more methodological details.

$$\tilde{y}_h = S\beta_h\hat{y}_h \quad (1)$$

The five reconciliation methods are briefly described below:

- **Bottom-Up (BU)**: naïvely sums the bottom forecasts to obtain the forecast at the top of the hierarchy. The forecasts at the top of the hierarchy, which are generally more accurate due to smoothing, are not used.
- **Minimum Trace error (MinT)**: The sum of the variances of the h-step ahead reconciled forecast is minimized, and all hierarchical levels are used. This method minimizes the error variance of the reconciled forecasts in expectation, so the reconciliation performance obtained should be optimal on average. However a requirement is that base forecasts should be unbiased [8].
- **Ordinary Least Squares (OLS)**: simplified version of MinT which minimizes the deviation obtained by the projection of summation constraints
- **Weighted Least Squares (WLS)**: The covariance matrix is simplified to the diagonal matrix of the base forecast errors
- **Hierarchical Least Squares (HLS)**: The covariance matrix is formed according to the structure of the hierarchy instead of the base forecast errors

CASE STUDY

A power distribution grid with both MV and LV levels is considered (cf. Figure 3). This power grid interfaces conventional demand and PV generation at various points of the network, which compose the nodal injections flowing in this system. It is assumed here that the only source of uncertainty is PV, i.e. load is taken as certain. This is obviously simplistic, but allows to isolate the contribution of renewable uncertainty to the flexibility potential of an MV grid.

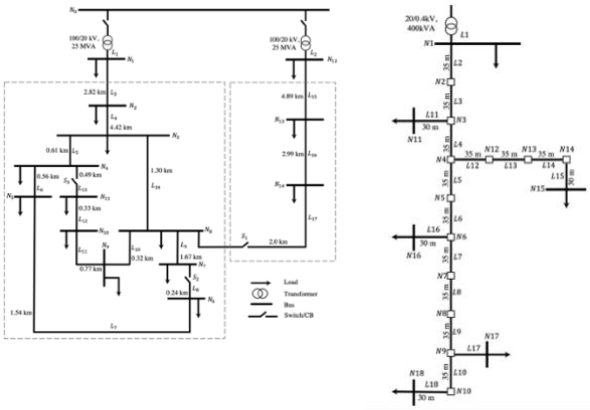

Figure 3: Architecture of the tested MV grid (left)) where PV production sites are located in several downstream LV grids of identical topology (right). Grid topology and parameters are from CIGRE' Task Force C6.04.02'

RESULTS

Hierarchical forecasts

Table 1 (left) shows that in terms of Mean Bias Error (MBE) RF tends to outperform Lasso at larger forecast horizons and benefits from using clear sky normalization, whereas this is not the case with Lasso. Interestingly, all reconciliation methods generally add to MBE as the forecast horizon increases. In the case of MinT, this may be expected because it is based on the assumption that the base forecasts are unbiased, which is not true in this case. Table 1 shows that, overall, the differences between the reconciliation methods are not substantial although there are occasions where a single method has noticeably lower score than the others.

Horizon	Clear sky	Lasso	Random Forest	BU	OLS	WLS	HLS	MinT
1	FALSE	-0.016	(-)	-0.022	-0.017	-0.021	-0.019	-0.021
1	TRUE	0.084	(-)	0.104	0.086	0.1	0.094	0.096
1	FALSE	(-)	0.093	0.079	0.091	0.082	0.086	0.083
1	TRUE	(-)	0.037	0.094	0.043	0.081	0.065	0.081
6	FALSE	0.376	(-)	0.361	0.375	0.364	0.369	0.373
6	TRUE	0.427	(-)	0.49	0.434	0.48	0.459	0.413
6	FALSE	(-)	0.422	0.534	0.434	0.516	0.478	0.545
6	TRUE	(-)	0.169	0.282	0.182	0.264	0.226	0.301
24	FALSE	0.599	(-)	0.608	0.6	0.606	0.603	0.601
24	TRUE	0.838	(-)	0.926	0.847	0.912	0.882	0.782
24	FALSE	(-)	0.417	0.538	0.431	0.52	0.478	0.552
24	TRUE	(-)	0.486	0.616	0.501	0.596	0.551	0.595

Horizon	Clear sky	Lasso	Random Forest	BU	OLS	WLS	HLS	MinT
1	FALSE	6.532	(-)	6.524	6.531	6.525	6.526	6.525
1	TRUE	6.206	(-)	6.215	6.206	6.211	6.208	6.209
1	FALSE	(-)	6.372	6.394	6.367	6.376	6.365	6.373
1	TRUE	(-)	6.127	6.139	6.123	6.126	6.119	6.127
6	FALSE	10.652	(-)	10.683	10.653	10.674	10.661	10.654
6	TRUE	10.82	(-)	10.98	10.831	10.946	10.883	10.803
6	FALSE	(-)	10.121	10.022	10.09	10.009	10.019	10.035
6	TRUE	(-)	9.585	9.501	9.562	9.495	9.507	9.514
24	FALSE	10.979	(-)	11.021	10.982	11.012	10.995	10.984
24	TRUE	12.202	(-)	12.432	12.22	12.388	12.298	12.137
24	FALSE	(-)	10.977	10.814	10.94	10.813	10.846	10.82
24	TRUE	(-)	11.099	10.923	11.058	10.922	10.957	10.923

Table 1: MBE (left) and RMSE (right) of unreconciled forecasts obtained from Lasso and PF and their reconciled variants

Estimation of the power flow at the TSO/DSO interface

Power flow analyses are first computed by using deterministic values (i.e., measurements) of the nodal injections to establish a reference scenario with grid's ``ground-truth" grid quantities. Then, nodal injections are replaced with forecasted series: grid quantities are recomputed and compared against the reference scenario.

The estimation of the power flow at the interface is summarized for three different weather conditions in Table 3. It shows that, as for the case of forecasting performance, no dominant model emerges in terms of estimation of the power flow at the TSO/DSO interface.

Deriving a predictive flexibility map

Although the estimated power flow at the interface is accurate on average, high errors may occur as in the case of Figure 4. Here PV forecasts errors reach up to 30% at bottom level and 10% at top level. This impacts the quantification of flexibility potential as shown in Figure 4. Here, an AC OPF derives the boundaries of active and reactive power at the TSO/DSO interface as a function of the PV forecasts at the site level. Flexibility is assumed to be provided by PV curtailment only (100% nominal power) and a modest flexibility in reactive power (6.67% nominal power [4]. Solving the OPF for different objectives of P-Q minimization/maximization gives an approximation of the flexibility map at the interface, see [4]-[5] for more details. A perfect forecast of PV would have led to a much higher flexibility envelope than the ones obtained with hierarchical forecasting. This illustrates the need to improve forecasts for distribution grids.

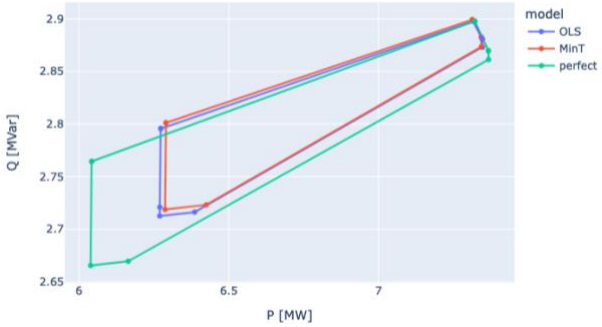

Figure 4: Flexibility map at the TSO/DSO interface with OLS, MinT reconciled forecasts and perfect forecasts (angle tolerance of 30° in the P-Q objective)

CONCLUSIONS

This study shows that using reconciled forecasts in load flow problems under PV uncertainty brings little improvement on average. However, there exist frequent occurrences of large forecasting errors which may pose a risk on the operational cost of MV grids that integrate flexible DER. In such cases, the impact on the flexibility potential at the TSO/DSO interface needs to be assessed.

In this work, it is assumed that all the data necessary for the predictive model is available, whereas it is commonplace that measurements or weather forecasts are missing in either the training or testing sets of predictive applications. The conditional stochastic optimization developed in [9] to optimally derive hierarchical forecasts in the case of missing data in the hierarchy could be

compared to the standard reconciliations presented in this work, which need to either ignore or impute records with missing values.

Another perspective consists in analyzing the temporal characteristics of the forecasting errors using reconciliation, to see if this may impact the quantification of flexibility which is itself affected by temporal couplings.

Acknowledgments

This work has been realized in the frame of the Smart4RES Project, a Research and Innovation Horizon 2020 program funded by the INEA agency under Grant Agreement n°864337.

The authors wish to thank ECMWF for the access to historical weather forecasts and SERGIES for the provision of renewable production data.

REFERENCES

[1] C. Di Modica, P. Pinson, and S. Ben Taieb, "Online forecast reconciliation in wind power prediction," Electr. Power Syst. Res., vol. 190, no. August 2020, p. 106637, 2021, doi: 10.1016/j.epsr.2020.106637.

[2] L. Nespoli, V. Medici, K. Lopatichki, and F. Sossan, "Hierarchical demand forecasting benchmark for the distribution grid," Electric Power Systems Research, vol. 189, p. 106755, Dec. 2020, doi: 10.1016/j.epsr.2020.106755.

[3] https://www.smart4res.eu/

[4] J. Silva, J. Sumaili, R. J. Bessa, L. Seca, M. Matos, and V. Miranda, "The challenges of estimating the impact of distributed energy resources flexibility on the TSO/DSO boundary node operating points," *Computers & Operations Research*, vol. 96, pp. 294–304, Aug. 2018, doi: 10.1016/j.cor.2017.06.004.

[5] M. Kalantar-Neyestanaki, F. Sossan, M. Bozorg, and R. Cherkaoui, "Characterizing the Reserve Provision Capability Area of Active Distribution Networks: A Linear Robust Optimization Method," *IEEE Transactions on Smart Grid*, vol. 11, no. 3, pp. 2464–2475, 2020, doi: 10.1109/TSG.2019.2956152.

[6] D. W. van der Meer, J. Widén, and J. Munkhammar, "Review on probabilistic forecasting of photovoltaic power production and electricity consumption," Renewable and Sustainable Energy Reviews, vol. 81. pp. 1484–1512, 2018, doi:10.1016/j.rser.2017.05.212.

[7] P. Bacher, H. Madsen, H. Aalborg Nielsen, "Online short-term solar power forecasting", Solar Energy, Volume 83, Issue 10, 2009, pp 1772-1783, https://doi.org/10.1016/j.solener.2009.05.016.

[8] S. L. Wickramasuriya, G. Athanasopoulos & R. J. Hyndman, "Optimal Forecast Reconciliation for Hierarchical and Grouped Time Series Through Trace Minimization", Journal of the American Statistical Association, 2019, 114:526, 804-819, DOI: 10.1080/01621459.2018.1448825

[9] A. Stratigakos, D. van Der Meer, S. Camal, G. Kariniotakis. End-to-end Learning for Hierarchical Forecasting of Renewable Energy Production with Missing Values. *17th International Conference on Probabilistic Methods Applied to Power Systems, PMAPS 2022*, Jun 2022, Manchester - Online, United Kingdom.

Horizon	Sky type	Lasso	Random forest	Random forest CS	Lasso BU	Random forest BU	Random forest CS BU	Lasso OLS	Random forest OLS	Random forest CS OLS	Lasso MinT	Random forest MinT	Random forest CS MinT
Active Power													
1	1	4.52%	**3.26%**	3.39%	4.52%	**3.26%**	3.39%	4.57%	3.31%	3.46%	4.53%	3.27%	3.40%
1	2	7.74%	7.52%	6.96%	7.74%	7.52%	6.96%	7.82%	7.34%	6.96%	7.75%	7.46%	**6.95%**
1	3	5.83%	5.40%	**4.64%**	5.83%	5.40%	**4.64%**	5.88%	5.37%	4.70%	5.84%	5.38%	4.65%
6	1	9.12%	6.40%	5.78%	9.12%	6.40%	5.78%	9.17%	6.33%	6.22%	9.17%	6.42%	**5.73%**
6	2	11.68%	10.35%	**9.57%**	11.68%	10.35%	**9.57%**	11.81%	10.21%	9.75%	11.79%	10.38%	9.58%
6	3	10.35%	9.38%	8.33%	10.35%	9.38%	8.33%	10.53%	9.40%	8.67%	10.51%	9.40%	**8.29%**
24	1	9.71%	8.09%	8.79%	9.71%	8.09%	8.79%	9.87%	**8.06%**	8.40%	9.85%	8.12%	8.71%
24	2	11.53%	**11.06%**	11.60%	11.53%	**11.06%**	11.60%	11.56%	11.26%	11.16%	11.55%	11.08%	11.48%
24	3	**10.61%**	10.71%	11.89%	**10.61%**	10.71%	11.89%	10.82%	11.04%	11.47%	10.80%	10.70%	11.79%
Reactive Power													
1	1	0.10%	**0.05%**	**0.05%**	0.10%	**0.05%**	**0.05%**	0.10%	0.06%	**0.05%**	0.10%	**0.05%**	**0.05%**
1	2	0.17%	0.15%	**0.13%**	0.17%	0.15%	**0.13%**	0.17%	0.15%	**0.13%**	0.17%	0.15%	**0.13%**
1	3	0.17%	0.15%	**0.12%**	0.17%	0.15%	**0.12%**	0.18%	0.15%	0.13%	0.18%	0.15%	**0.12%**
6	1	0.20%	0.11%	0.09%	0.20%	0.11%	0.09%	0.20%	0.11%	**0.08%**	0.20%	0.11%	0.09%
6	2	0.26%	0.21%	0.19%	0.26%	0.21%	0.19%	0.27%	0.20%	**0.17%**	0.27%	0.21%	0.19%
6	3	0.32%	0.27%	**0.23%**	0.32%	0.27%	**0.23%**	0.33%	0.27%	**0.23%**	0.33%	0.27%	**0.23%**
24	1	0.16%	**0.10%**	0.11%	0.16%	**0.10%**	0.11%	0.16%	**0.10%**	**0.10%**	0.16%	**0.10%**	0.11%
24	2	0.23%	0.20%	0.20%	0.23%	0.20%	0.20%	0.23%	0.20%	**0.19%**	0.23%	0.20%	0.20%
24	3	0.30%	**0.28%**	0.32%	0.30%	**0.28%**	0.32%	0.31%	0.29%	0.31%	0.31%	**0.28%**	0.32%
Voltage													
1	1	0.022%	**0.015%**	0.016%	0.022%	**0.015%**	0.016%	0.022%	**0.015%**	0.016%	0.022%	**0.015%**	0.016%
1	2	0.037%	0.036%	0.034%	0.037%	0.036%	0.034%	0.038%	0.035%	0.034%	0.037%	0.036%	**0.033%**
1	3	0.028%	0.026%	**0.022%**	0.028%	0.026%	**0.022%**	0.028%	0.025%	**0.022%**	0.028%	0.026%	**0.022%**
6	1	0.043%	0.030%	0.027%	0.043%	0.030%	0.027%	0.043%	0.029%	0.029%	0.043%	0.030%	**0.026%**
6	2	0.056%	0.049%	**0.045%**	0.056%	0.049%	**0.045%**	0.057%	0.049%	0.046%	0.057%	0.049%	**0.045%**
6	3	0.049%	0.044%	**0.039%**	0.049%	0.044%	**0.039%**	0.050%	0.044%	0.040%	0.050%	0.044%	**0.039%**
24	1	0.047%	**0.038%**	0.041%	0.047%	**0.038%**	0.041%	0.048%	**0.038%**	0.039%	0.048%	**0.038%**	0.040%
24	2	0.056%	**0.053%**	0.055%	0.056%	**0.053%**	0.055%	0.056%	0.054%	**0.053%**	0.056%	**0.053%**	0.054%
24	3	**0.050%**	**0.050%**	0.055%	0.050%	**0.050%**	0.055%	0.051%	0.051%	0.054%	0.051%	**0.050%**	0.055%
Current													
1	1	1.25%	**0.81%**	**0.81%**	1.25%	**0.81%**	**0.81%**	1.27%	**0.81%**	0.82%	1.26%	**0.81%**	0.82%
1	2	2.16%	2.03%	**1.81%**	2.16%	2.03%	**1.81%**	2.18%	2.01%	1.82%	2.16%	2.02%	**1.81%**
1	3	1.81%	1.61%	**1.34%**	1.81%	1.61%	**1.34%**	1.82%	1.59%	1.35%	1.81%	1.60%	**1.34%**
6	1	2.50%	1.62%	1.36%	2.50%	1.62%	1.36%	2.53%	1.55%	**1.26%**	2.52%	1.64%	1.38%
6	2	3.17%	2.80%	2.55%	3.17%	2.80%	2.55%	3.23%	2.77%	**2.41%**	3.22%	2.80%	2.58%
6	3	3.23%	2.87%	2.55%	3.23%	2.87%	2.55%	3.30%	2.84%	**2.51%**	3.29%	2.88%	2.56%
24	1	2.43%	1.62%	1.75%	2.43%	1.62%	1.75%	2.49%	**1.61%**	1.62%	2.49%	1.64%	1.73%
24	2	3.06%	2.80%	2.93%	3.06%	2.80%	2.93%	3.10%	2.81%	**2.71%**	3.09%	2.81%	2.88%
24	3	3.23%	**3.09%**	3.48%	3.23%	**3.09%**	3.48%	3.31%	3.16%	3.34%	3.30%	**3.09%**	3.45%

Table 2: Mean absolute error of the estimation errors of various grid quantities for different forecasting horizons and sky conditions (1: clear-sky; 2: partly cloudy; 3: overcast). Bold typeface denote the best performers along the columns.